

Numerical research orthotropic geometrically nonlinear shell stability using the mixed finite element method

L Stupishin¹, K Nikitin¹ and A Kolesnikov¹

¹ Urban, road Construction and Structural Mechanics Department, South-West State University, 305040, 50-let Otyabrya st., 94, Kursk, Russian Federation

lulgsh@yandex.ru

Abstract. A methodology for shell stability research and determining buckling load, based on the mixed finite element method are proposed. Axisymmetric geometrically nonlinear shallow shells made of orthotropic material are considered. The results of numerical research of stability by changing the shape of shells, ratio of elastic modulus of the material and parameters of the support contour are presented.

1. Introduction

The developed methodology is based on the Galerkin method and finite element method in a mixed formulation. This approach is described in the works [1, 2, 3], has several advantages over the classical formulation of the finite element method. Solution of the nonlinear problem is carried out using one of the algorithm continuation methods. The technique can be applied in various fields, including the analysis of nano-scale objects.

2. Description of the methodology

We used an algorithm continuation method [4], is as follows:

$$\begin{aligned} \xi_k^0 &= t \cdot dX_{k-1}, \quad X_k^0 = X_{k-1} + \xi_k^0, \\ \begin{cases} J(X_k^i) \Delta X_k^{i+1} = -F(X_k^i) \\ (\xi_k^i, \Delta X_k^{i+1}) = \frac{1}{2}(t^2 - (\xi_k^i, \xi_k^i)) \end{cases}, \\ X_k^{i+1} &= X_k^i + \Delta X_k^{i+1}, \quad \xi_k^{i+1} = X_k^{i+1} - X_{k-1}, \end{aligned} \quad (1)$$

where, $F(X)$ - nonlinear system of n equations with $n+1$ unknown variables what is solved; X - vector of unknown variables. In our problem it includes a system of nodal degrees of freedom and the parameter of loading q . The system of equations $F(X)$ has a set of solutions that can be represented by curve solutions; k - 0, 1, 2 ... - number of step along the curve solutions; i - 0, 1, 2 ... - the number of refinement iteration at each step k ; $F(X_k^i)$ and X_k^i - respectively is system of equations and vector of its solutions at step k and refinement iteration i ; ξ_k^0 - initial direction vector for search a solution X_k^i at step k ; t - the step value; dX_k - unit vector tangent to the curve solutions at current step k ; dX_{k-1} - unit vector tangent to the



curve solutions at previous step; X_k^0 - initial vector of solution of system equation $F(X_k^i)$ at step k ; X_{k-1} - last refined vector of solution of system equation $F(X_k^i)$ at previous step; $J(X_k^i)$ - Jacobi matrix system of equations $F(X_k^i)$ at step k and refinement iteration i ; ξ_k^i - direction vector for search a solution X_k^i at step k and refinement iteration i ; ΔX_k^i - vector of iterative refinement of solution vector X_k^i at step k and refinement iteration i ; X_k^{i+1} - refined vector of solution of system equation $F(X_k^i)$ at step k and refinement iteration i ; ξ_k^i - refined direction vector for search a solution X_k^i at step k and refinement iteration i .

Refinement is being until the following conditions hold:

$$\|\Delta X_k^{i+1}\| > \varepsilon, \quad (2)$$

where, ε - constant that specifies the search accuracy solutions.

The value of dX_k is determined by solving the system of equations of the form:

$$\begin{cases} J(X_k) dX_k = 0 \\ (dX_k, dX_k) = 1 \end{cases}. \quad (3)$$

To determine the stress-strain state of the shell used finite element method, matrices and vectors which are derived using Galerkin method. An expression describing the state of the j -th finite element is of the form:

$$F_j(X_{k,j}^i) = \{r_1 \quad r_2 \quad r_3 \quad r_4\}^T, \quad (4)$$

where,

$$\begin{aligned} r_1 = & \left(\frac{\eta - \chi}{3} \bar{C}_2 + \chi \bar{C}_{12} - e_1 \bar{C} \right) \Phi_1 + e_3 \theta_1 + \left(e_1 \bar{C}_1 + \frac{\eta - \chi}{6} \bar{C}_2 \right) \Phi_2 + e_4 \theta_2 + \\ & + (\eta^2 + 3\chi\eta - 4\chi^2) \frac{\theta_1^2}{40} + (2\eta^2 + \chi\eta - 3\chi^2) \frac{\theta_1 \theta_2}{60} + (3\eta^2 - \chi\eta - 2\chi^2) \frac{\theta_2^2}{120}, \end{aligned} \quad (5)$$

$$\begin{aligned} r_2 = & -e_3 \Phi_1 + \left(\frac{\eta - \chi}{3} \bar{D}_2 - \chi \bar{D}_{12} - e_1 \bar{D}_1 \right) \theta_1 + e_4 \Phi_2 + \left(e_1 \bar{D}_1 + \frac{\eta - \chi}{6} \bar{D}_2 \right) \theta_2 - \\ & - \frac{qhC\sqrt{\mu}}{120} (-8\chi^4 + 7\eta^2\chi^2 + 7\eta\chi^3 - 3\eta^3\chi - 3\eta^4) - \frac{s_i}{6} (\eta^2 + \eta\chi - 2\chi^2) + \\ & + (4\chi^2 - 3\chi\eta - \eta^2) \frac{\theta_1 \Phi_1}{20} + (3\chi^2 - \chi\eta - 2\eta^2) \frac{\theta_2 \Phi_1}{60} + (3\chi^2 - \chi\eta - 2\eta^2) \frac{\theta_1 \Phi_2}{60} + \\ & + (2\chi^2 + \chi\eta - 3\eta^2) \frac{\theta_2 \Phi_2}{60}, \end{aligned} \quad (6)$$

$$\begin{aligned} r_3 = & \left(e_2 \bar{C}_1 + \frac{\eta - \chi}{6} \bar{C}_2 \right) \Phi_1 + e_4 \theta_1 + \left(\frac{\eta - \chi}{3} \bar{C}_2 + \eta \bar{C}_{12} - e_2 \bar{C}_1 \right) \Phi_2 - e_3 \theta_2 + \\ & + (4\eta^2 - 3\chi\eta - \chi^2) \frac{\theta_2^2}{40} + (3\eta^2 - \chi\eta - 2\chi^2) \frac{\theta_1 \theta_2}{60} + (2\eta^2 + \chi\eta - 3\chi^2) \frac{\theta_1^2}{120}, \end{aligned} \quad (7)$$

$$r_4 = e_4 \Phi_1 + \left(e_2 \bar{D}_1 + \frac{\eta - \chi}{6} \bar{D}_2 \right) \theta_1 + e_3 \Phi_2 + \left(\frac{\eta - \chi}{3} \bar{D}_2 + \eta \bar{D}_{12} - e_2 \bar{D}_1 \right) \theta_2 -$$

$$\begin{aligned} & \frac{qhC\sqrt{\mu}}{120}(-7\chi^4 + 23\eta^2\chi^2 - 7\eta\chi^3 - 7\eta^3\chi - 12\eta^4) - \frac{s_i}{6}(2\eta^2 - \eta\chi - \chi^2) + \\ & + (\chi^2 + 3\chi\eta - 4\eta^2)\frac{\theta_2\Phi_2}{20} + (2\chi^2 + \chi\eta - 3\eta^2)\frac{\theta_1\Phi_2}{60} + (3\chi^2 - \chi\eta - 2\eta^2)\frac{\theta_1\Phi_1}{60} + \\ & + (2\chi^2 + \chi\eta - 3\eta^2)\frac{\theta_2\Phi_1}{60}, \end{aligned} \quad (8)$$

$$e_1 = \frac{\eta^2 + \eta\chi + 4\chi^2}{6(\chi - \eta)}, \quad e_2 = \frac{4\eta^2 + \eta\chi + \chi^2}{6(\chi - \eta)}, \quad e_3 = \frac{K}{12}(\eta^2 + 2\eta\chi - 3\chi^2), \quad e_4 = \frac{K}{12}(\eta^2 - \chi^2), \quad (9)$$

$$X_{k,j}^i = \{\Phi_1, \theta_1, \Phi_2, \theta_2, q\}^T, \quad (10)$$

χ & η - respectively radial coordinate the start and end node of the j-th axisymmetric finite element of shell, $X_{k,j}^i$ - vector, which includes the of all the degrees of freedom nodes of a finite element.

Other details relating to used of the mixed finite element including assembly algorithm generalized matrix given in [1 - 3].

Designed calculation algorithm determines the stress-strain state of the shell at each step of the method of continuation on parameter. In the process of calculating the deformation analysis of its changes and fixes their extreme values. According to it determines the values of the upper and lower buckling loads corresponding to the upper and lower extreme point on the graph of the deformation of the load (i.e., the upper and lower at the turning point).

3. Checking the results

The results of calculations were compared for the values of the upper and lower buckling loads at [5]. The difference in the values is not more than 1.2%.

To establish the convergence of the algorithm was carried out test calculations for different finite element mesh density in the radial direction. The results show convergence forces, moments and displacements with increasing density of the grid. Acceptable for practical calculations results are obtained by partitioning the shell at least 20 elements in the radial direction.

4. Investigation of stability

The developed methodology was used to study the influence on the values of the upper and lower buckling loads of the following parameters:

- parameter that specifies the shape of the shell (parameter Z);
- parameters of elastic fastening support contour the shell (parameters n and m);
- the ratio of the elastic modulus of the shell material in the radial (E_1) and circumferential direction (E_2) (parameter Θ).

Shape generatrix a shell of revolution is defined by the function parameter Z:

$$f(\bar{\rho}) = f_{\max}\rho^Z, \quad (11)$$

where, f_{\max} - the rise in the center of the shell, ρ - dimensionless coordinate, which changes from 0 in the center of the shell to the value 1 on the support contour.

It is assumed that the shell is based on the elastic support contour, which specifies the parameters of the flexibility n and m. Parameter n describes flexibility of the support contour in the radial direction, and may range from -0.3 (when displacement in the radial direction are prevented) to infinity (if not restricted displacement in a radial direction). The parameter m describes flexibility of the support contour in its torsion and may range from +0.3 (if the

reference contour is a hinge and rotation not restricted) to infinity (if the rotation of the support contour are prevented).

In carrying out investigations, the parameters varied the shell in the following ranges: Z - from 1 to 2.5; n - from -0.3 to 100; m - from 0.3 to 100. Considered shallow shell of revolution with base radius $a = 1$ [m] and height $f_{\max} = 1$ [m]; thickness $h = 4$ [mm], Poisson's ratio of the shell material $\nu_1 = \nu_2 = 0.3$. The shell is loaded uniformly distributed load of intensity p .

Some results are shown in Fig. 1 and Fig. 4, which presents graphs of the dimensionless deflection depending on the values of the load on the shell and the values of variable parameters. Fig. 2, Fig. 3, Fig. 5 and Fig. 6 are graphs of the upper and lower buckling loads, depending on the values of the variable parameters of the shell.

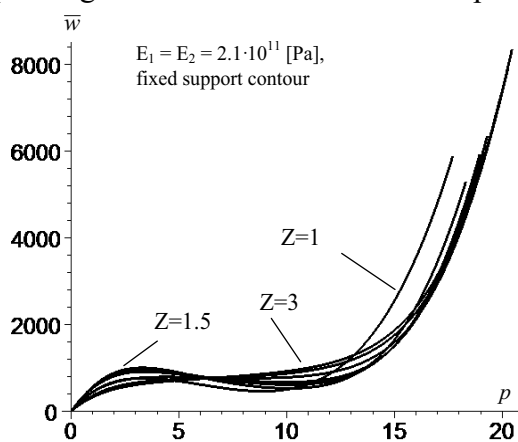


Figure 1. The graph change dimensionless displacements in the center of the shell when the value of the load p for different values of Z .

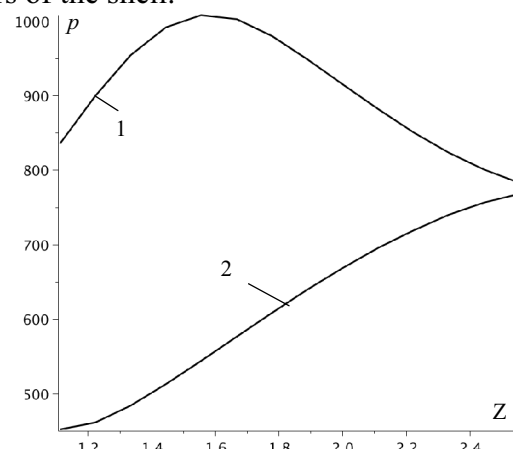


Figure 2. The graphs change the values of buckling loads p , depending on the value of Z (1 - upper buckling load 2 - lower buckling load).

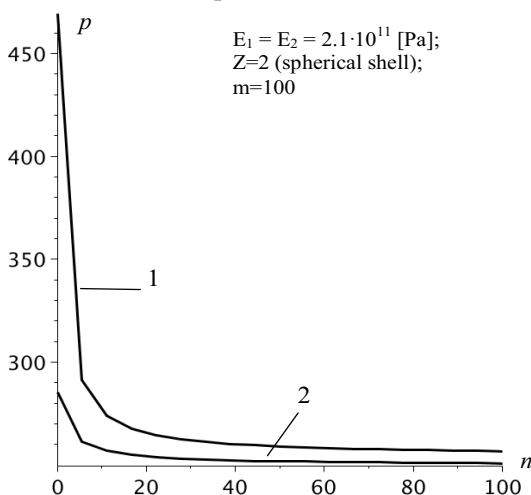


Figure 3. The graphs change the values of buckling loads, depending on the value of n (1 - upper buckling load 2 - lower buckling load).

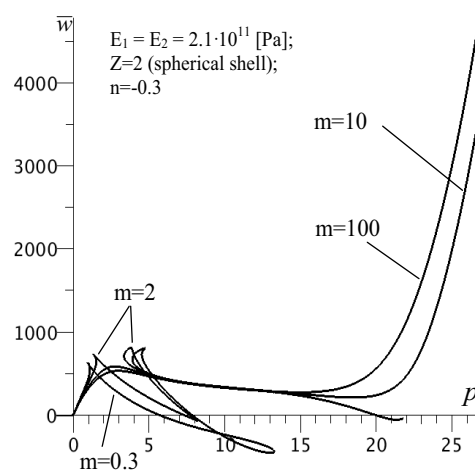


Figure 4. The graphs change dimensionless displacements in the center of the shell when the value of the load p for different values of m

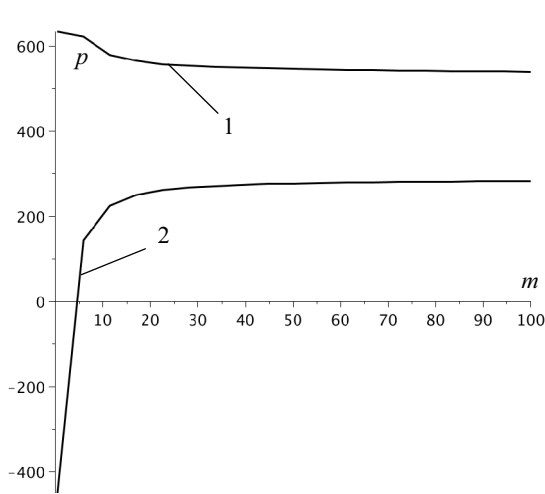


Figure 5. The graphs change the values of buckling loads, depending on the value of m (1 - upper buckling load 2 - lower buckling load).

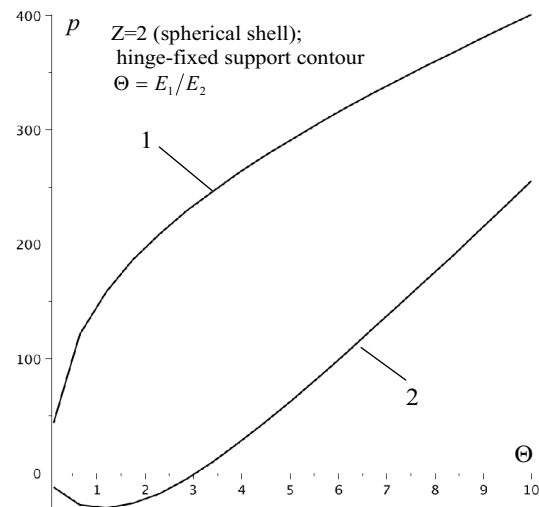


Figure 6. The graphs change the values of buckling loads, depending on the value of Θ (1 - upper buckling load 2 - lower buckling load).

When you change the Z observed extreme values of the upper buckling load which is located near $Z = 1.6$ (see Fig. 2). We can assume that the shell of such forms have the highest safety factor than other forms of the shell under the influence of uniformly distributed loads. At the same time, the extremum for the lower buckling load is absent. By increasing the shape parameter Z is observed only increase the values of the lower buckling load (Fig. 2). The largest gap between the values of the upper and lower buckling loads occurs precisely at the point of extremum upper buckling load.

Change the parameters n and m shows the growth of buckling load with an increase in the stiffness of the support contour the radial direction and increase flexibility in respect of the rotation (Fig. 3, Fig. 5). The highest values of buckling loads correspond to the hinge-fixed the support contour.

Increasing the parameter Θ results in an increase the upper buckling load (Fig. 6). At the same time, with $\Theta = 1$ there is an extreme value of the lower buckling load.

5. Conclusions

Developed methodology based on mixed finite element method shows good accuracy and convergence of the results. It is more effective in comparison with finite elements in other formulations. Applying the methodology of investigating the shell's stability allows you to find more optimal combination of size, shape for the shell and the parameters of it's of the support contour. Presented methodology may be used for building and analysis of nano-scale objects in matereals.

This work was supported by the grant of the President of the Russian Federation #MK-9203.2016.8

References

- [1] Stupishin L and Nikitin K 2014 *Adv. Mat. Res.* **919-921**, pp 1299-1302
- [2] Stupishin L and Kolesnikov A 2014 *Appl. Mech. & Mat.* **501-504**, pp 766-769
- [3] Stupishin L and Nikitin K 2014 *Appl. Mech. & Mat.* **501-504**, pp 514-517
- [4] Grigolyuk E. and Shalashilin V. 1988 *Problems of nonlinear deformation* (Moscow: Nauka Publ)
- [5] Valishvili N 1976 *Methods of analyzing shells of revolution on electronic digital computers* (Moscow: Mashinostroenie Publ)